pp 429–445. © Royal Aeronautical Society 2019
doi:10.1017/aer.2019.121

A robust hybrid nonlinear guidance law for intercepting a non-cooperative maneuvering target

Xiaodong Yan and Shi Lyu
yan804@nwpu.edu.cn
Shaanxi Key Laboratory of Aerospace Flight Vehicle Technology
Northwestern Polytechnical University,
Xi'an
China

ABSTRACT

This paper has proposed a new robust hybrid nonlinear guidance law, which accounts for a missile's terminal line-of-sight (LOS) angle constraint, in order to intercept a non-cooperative maneuvering target. The proposed hybrid nonlinear guidance strategy consists of two phases; in the first phase, a guidance law named PIGL is derived from prescribed performance control and the inertial delay control method. In PIGL, a revised prescribed performance function is put forward, and a prescribed performance controller with unknown uncertainties is then derived. The controller smoothly drives both the LOS angle and its rate to a predesigned small region under unknown uncertainties that are induced by target's maneuvers within a fixed time. Then, a guidance law named SIGL is activated, which is derived from sliding mode control and inertial delay control. By driving the desired sliding mode variable to zero within a finite time, the SIGL guidance law is able to achieve high terminal interception accuracy. The robustness of both of the proposed sub-guidance laws has been proved explicitly in this paper. The hybrid guidance law has the advantage of a tunable convergence rate of the LOS angle and the rate of the LOS angle at the beginning period, by which an excessive large initial maneuver can be avoided. Meanwhile, the hybrid guidance law also has the advantage of lower sensitivity to errors in the estimation of the time-to-go.

Keywords: Prescribed performance control; Sliding mode control; Inertial delay control; Terminal angle constraint; Interception guidance

NOMENCLATURE

T	the target
M	the missile
V_M	missile velocity

Received 13 May 2019; revised 11 August 2019; accepted 21 August 2019.

A_M missile acceleration
γ_M flight path angle of the missile
V_T target velocity
A_T target acceleration
γ_T flight path angle of the target
R distance between the target and the missile
λ LOS angle between the target and the missile
A_{TR} target's acceleration along the LOS
$A_{T\lambda}$ target's acceleration normal to the LOS
s_x sliding mode variable
ρ prescribed performance variable
u_ρ virtual control command
t_d predetermined time constant
β weighting parameter
t_{go} estimated time-to-go

1.0 INTRODUCTION

Intercepting non-cooperative maneuvering targets is a very important task when constructing an effective defense system. In decades past, many contributions have been made to the design of advanced terminal homing guidance laws based on prescribed performance control (PPC)[1], feedback linearization control[2], nonlinear H_∞ control[3], proportional navigation[4], and so on. These guidance laws accomplished highly accurate interception by eliminating the zero-miss distance and reducing the line-of-sight (LOS) angle rate to zero. Furthermore, interception probability of the missile being intercepted is enhanced by imposing an additional terminal impact angle constraint in these guidance laws.

Although effective, the interception accuracy of these model-based guidance laws may deteriorate where modeling errors and uncertainties exist. To solve this issue, sliding mode control (SMC) was proposed[5–7] due to its ability to inhibit any modeling errors and uncertainties[8]. To improve the SMC's performance, the disturbance observer[9,10] and the extended state observer[11,12] have been generally applied to estimate the uncertainties. Although the effectiveness has been verified, additional parameters have been introduced which were predesigned for the observer, and the estimated parameters often have large and abrupt changes. Recently, the inertial delay control (IDC) method was proposed to assure the continuity of the estimate, even without knowing the bounds of uncertainties in advance[6,13]. However, these SMC-based guidance laws usually generate large discontinuous commands in the homing phase even if IDC is used[14]. On the one hand, a portion of the guidance law with fixed control gains are proportional to the sliding mode variable, which is often initialized with a large value at the begin period. The saltation of guidance commands cannot be avoided once the guidance law is switched on. On the other hand, when an unexpected maneuver is performed by a non-cooperative target, the observers will produce an abruptly changed output, which induces discontinuous guidance commands. The sudden changes of the guidance commands is undesirable due to the limitation of the control system, as well as the short flight time in the terminal homing phase[15]. Therefore, SMC-based guidance laws still need to be improved in order to deal with the challenge of sensitivity to the initial conditions and the uncertainty induced by the target's maneuvers.

On consideration of the above content, a robust hybrid nonlinear guidance law has been proposed in this paper. Firstly, a new time-varying continuous prescribed performance function

https://doi.org/10.1017/aer.2019.121 Published online by Cambridge University Press

(PPF) was constructed in the prescribed performance controller. Then, based on the new proposed PPF, a novel PPC-type guidance law was derived to drive both the LOS angle and its rate to a predesigned small region with unknown uncertainties. The new PPC-type guidance law is able to mitigate extremely abrupt changes of the guidance commands, especially, at the initial period of the homing phase. Secondly, in order to overcome the limitations of time-dependence and the bounded convergence of the sliding mode variable, an improved SMC and IDC-based guidance law has been developed to theoretically drive the desired sliding mode variable to zero within a finite time. Accordingly, the proposed hybrid guidance law has the properties of tunable transient performance of the guidance commands and is able to achieve high interception accuracy.

2.0 PROBLEM STATES

2.1 Modeling

In the current work, Fig. 1 has shown a scenario where an interception missile is approaching a maneuvering target. M denotes the missile while T denotes the target, the distance from M to T is denoted by R. The line-of-sight (LOS) angle between M and T is λ, and V_M denotes the velocity of M while V_T denotes the velocity of T Moreover, the accelerations of M and T are denoted by A_M and A_T, respectively. Meanwhile, the flight path angles of M and T are denoted by γ_M and γ_T, respectively.

Assuming the velocities of M and T are non-varying and have constant values, the M-T relative kinematics of the engagement can be formulated from[14]

$$\dot{R} = V_T \cos(\gamma_T - \lambda) - V_M \cos(\gamma_M - \lambda) < 0 \quad \ldots (1)$$

$$\dot{\lambda} = \frac{1}{R}[V_T \sin(\gamma_T - \lambda) - V_M \sin(\gamma_M - \lambda)] \quad \ldots (2)$$

$$\dot{\gamma}_M = \frac{A_M}{V_M} \quad \ldots (3)$$

$$\dot{\gamma}_T = \frac{A_T}{V_T} \quad \ldots (4)$$

From Eq. (1) and Eq. (2)[14], the derivative of $\dot{R}$ and $\dot{\lambda}$ can be derived as follows:

$$\ddot{R} = R\dot{\lambda}^2 + A_{TR} - A_M \sin(\lambda - \gamma_M) \quad \ldots (5)$$

$$\ddot{\lambda} = -\frac{2\dot{R}\dot{\lambda} - A_{T\lambda} + A_M \cos(\lambda - \gamma_M)}{R} \quad \ldots (6)$$

where $A_{TR} = A_T \sin(\lambda - \gamma_T)$ represents the target's acceleration along the LOS, and $A_{T\lambda} = A_T \cos(\lambda - \gamma_T)$ represents the target's acceleration normal to the LOS. Here, a new variable h is defined as:

$$h = A_M + A_{T\lambda} - A_M \cos(\lambda - \gamma_M) \quad \ldots (7)$$

Consequently, the angle rate dynamics from Eq. (6) of the LOS can be rewritten as

$$\ddot{\lambda} = -\frac{2\dot{R}\dot{\lambda} - h + A_M}{R} \quad \ldots (8)$$

https://doi.org/10.1017/aer.2019.121 Published online by Cambridge University Press

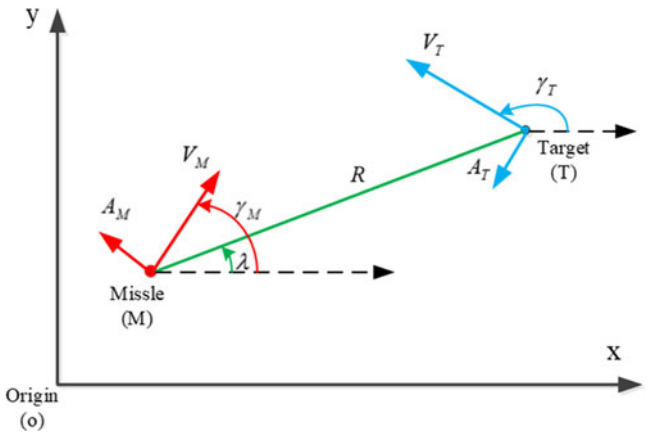

Figure 1. Schematic of terminal homing engagement.

On account of the non-cooperative nature of the target, $A_{T\lambda}$ is obviously unknown for the interception missile in advance. Therefore, the variable h can be taken as a model uncertainty and can be assumed to be bounded with the form as[14]:

$$\left|\frac{d^j h}{dt^j}\right| \le \mu \quad j = 0,\ 1,\ 2,\ ...,\ n \qquad \ldots (9)$$

where μ is an unknown positive constant.

2.2 The linear sliding mode manifold for the state errors

Considering a system such as

$$\ddot{x} = f(x, \dot{x}, t) + g(x, \dot{x}, t)u \qquad \ldots (10)$$

In Eq. (10), $f(x, \dot{x}, t)$ and $g(x, \dot{x}, t)$ are known functions, u is the control input.

A linear sliding mode manifold can be defined as[16]:

$$s_x = \dot{x} + kx = 0, \quad k > 0 \qquad \ldots (11)$$

where s_x is a sliding mode variable. If $s_x = 0$, the system states x and $\dot{x}$ will be asymptotically driven to zero[16].

As stated in the literatures[17,18], the interception guidance law for a missile determines the guidance commands needed to control the missile to capture the target with a predesigned LOS angle λ_d if the value of R is lower than a constant value R_f. Accordingly, the LOS angle error of the missile is yielded as $e_\lambda = \lambda - \lambda_d$. Moreover, the angle error dynamics is yielded by as per the literatures[17,18]

$$\ddot{e}_\lambda = \ddot{\lambda} = -\frac{2\dot{R}\dot{\lambda} - h + A_M}{R} \qquad \ldots (12)$$

According to Eq. (11), a sliding mode variable can be determined as:

$$s_e = \dot{e}_\lambda + ke_\lambda \qquad \ldots (13)$$

https://doi.org/10.1017/aer.2019.121 Published online by Cambridge University Press

and its derivative is yielded as

$$\dot{s}_e = \ddot{e}_\lambda + k\dot{e}_\lambda = -\frac{2\dot{R}\dot{\lambda} - h + A_M}{R} + k\dot{e}_\lambda \quad \ldots (14)$$

3.0 DESIGNING THE TERMINAL HOMING GUIDANCE LAW

3.1 PPC and IDC-based guidance law (PIGL)

Since the performance of guidance commands is coupled to the convergence rate of the sliding mode variable, a prescribed performance controller with a revised PPF, which inherits the initial time-varying properties of the sliding mode variable, can enhance the transient performance of commands, such as, avoiding large sudden changes in the guidance commands. Accordingly, an equivalent second-order system can be constructed as[19]:

$$\begin{cases} \dot{\rho} = u_\rho \\ \dot{u}_\rho = u_{jerk} \end{cases} \quad \ldots (15)$$

where ρ is the prescribed performance variable (PPV) and is treated as an equivalent system state, u_ρ is the virtual control command and is also treated as another equivalent system state, u_{jerk} represents the virtual jerk. An optimal cost function can be defined as follows:

$$\min J = \int_0^{t_d} \left((t - t_d/\beta)^2 + 1\right)^{-1} u_{jerk}^2 \Big/ 2dt \quad \ldots (16)$$

where t_d is a predetermined time, and β is a weighting parameter used to adjust the characteristics of u_ρ. The boundary conditions of the equivalent second-order system are $\rho|_{t=0} = s_0$, $\rho|_{t=t_d} = s_d$, $u_\rho\big|_{t=0} = u_{\rho 0}$, $u_\rho\big|_{t=t_d} = u_{\rho d}$, where s_0 is the initial value of s_e, $u_{\rho 0}$ is the initial value of the approximate derivative of the sliding mode variable $\hat{\dot{s}}_e$ without considering the unknown uncertainty h, $u_{\rho d}$ is the predesigned virtual control command at $t = t_d$, and s_d is a predetermined value of s at $t = t_d$.

The Hamilton function of the optimal problem can be written as:

$$H = \lambda_\rho u_\rho(t) + \lambda_{u_\rho} u_{jerk} + \left((t - t_d/\beta)^2 + 1\right)^{-1} u_{jerk}^2/2 \quad \ldots (17)$$

where λ_ρ and λ_{u_ρ} are covariant variables.

As per the literature[20], the solutions are as follows:

$$\dot{\lambda}_\rho = -\frac{\partial H}{\partial \rho} = 0 \Rightarrow \lambda_\rho = a_1 \quad \ldots (18)$$

$$\dot{\lambda}_{u_\rho} = -\frac{\partial H}{\partial u_\rho} = -\lambda_\rho \Rightarrow \lambda_{u_\rho} = -a_1 t + a_2 \quad \ldots (19)$$

$$\frac{\partial H}{\partial u_{jerk}} = \left((t - t_d/\beta)^2 + 1\right)^{-1} u_{jerk} + \lambda_{u_\rho} = 0 \Rightarrow u_{jerk} = -\left((t - t_d/\beta)^2 + 1\right)\lambda_{u_\rho} \quad \ldots (20)$$

https://doi.org/10.1017/aer.2019.121 Published online by Cambridge University Press

Consequently, the general solutions for u_ρ and ρ are as follows:

$$u_\rho = a_3 - \left(a_2 + \frac{a_2 t_d^2}{\beta^2}\right)t + \left(\frac{a_1}{2} + \frac{a_2 t_d}{\beta} + \frac{a_2 t_d^2}{2\beta^2}\right)t^2 - \left(\frac{a_2}{3} + \frac{2a_1 t_d}{3\beta}\right)t^3 + \frac{a_1 t^4}{4} \quad \ldots (21)$$

$$\rho = a_4 + a_3 t - \frac{1}{2}\left(a_2 + \frac{a_2 t_d^2}{\beta^2}\right)t^2 + \frac{1}{3}\left(\frac{a_1}{2} + \frac{a_2 t_d}{\beta} + \frac{a_2 t_d^2}{2\beta^2}\right)t^3 - \frac{1}{4}\left(\frac{a_2}{3} + \frac{2a_1 t_d}{3\beta}\right)t^4 + \frac{a_1 t^5}{20} \quad \ldots (22)$$

Accordingly, with t increasing from 0 to t_d, the coefficients a_1, a_2, a_3 and a_4 are determined by the boundary conditions of u_ρ and ρ.

A transformed error z can be defined as follows[1].

$$z = \ln\left(\frac{s_e/\rho - M_{\min}}{M_{\max} - s_e/\rho}\right) \quad \ldots (23)$$

where $M_{\max} > 2$ and $M_{\min} = 2 - M_{\max}$. When s_0 and s_d are nonzero and they both have the same sign, an appropriate value of β in Eq. (22) should be chosen to avoid ρ being zeroed in Eq. (23). In reality, at the beginning of terminal homing phase, s_0 always satisfies or could be controlled as $|s_0| \geq \varepsilon_s$, where ε_s has a small positive value.

In Eq. (23), if z asymptotically converges to zero, s_e will also asymptotically converge to ρ. The derivative of z is yielded as follows:

$$\dot{z} = \frac{C}{\rho^2}(\dot{s}_e\rho - \dot{\rho}s_e) \quad \ldots (24)$$

where

$$C = \frac{M_{\max} - M_{\min}}{(s_e/\rho - M_{\min})(M_{\max} - s_e/\rho)} \quad \ldots (25)$$

A Lyapunov function v can be constructed as:

$$v = \frac{1}{2}z^2 \quad \ldots (26)$$

Substituting Eq. (12) and Eq. (14) into Eq. (24) yields $\dot{z}$ as follows:

$$\dot{z} = \frac{C}{\rho^2}\left[\left(-\frac{2\dot{R}\dot{\lambda} - h + A_M}{R} + k\dot{e}_\lambda\right)\rho - \dot{\rho}s_e\right] \quad \ldots (27)$$

A_M can be defined as:

$$A_M = -R\left(u_{eq_1} + \frac{\rho}{C}u_2\right) \quad \ldots (28)$$

where

$$u_{eq_1} = \frac{2\dot{R}\dot{\lambda}}{R} + \frac{\dot{\rho}}{\rho}s_e - k\dot{e}_\lambda \quad \ldots (29)$$

https://doi.org/10.1017/aer.2019.121 Published online by Cambridge University Press

and h_1 can be defined as:

$$h_1 = \frac{Ch}{\rho R} \quad \ldots (30)$$

Substituting Eqs. (28), (29) and (30) into Eq. (27), the revised term $\dot{z}$ is yielded as follows:

$$\dot{z} = h_1 + u_2 \quad \ldots (31)$$

h_1 is passed through a broadband filter $G_f(s)$, such as[13]:

$$G_f(s) = \frac{1}{\tau s + 1} \quad \ldots (32)$$

where τ is a constant. The dynamics of the estimate of h_1 is yielded as:

$$\tau \dot{\hat{h}}_1 + \hat{h}_1 = \dot{z} - u_2 \quad \ldots (33)$$

If u_2 is designed as

$$u_2 = -k_z z - \hat{h}_1 \quad \ldots (34)$$

Then Substituting Eq. (34) into Eq. (33) yields the following:

$$\tau \dot{\hat{h}}_1 = \dot{z} + k_z z \quad \ldots (35)$$

Integrating both sides of Eq. (35) yields the following:

$$\hat{h}_1 = \hat{h}_1\Big|_{t=0} + \frac{1}{\tau}\left(z - z|_{t=0} + \int_0^t k_z z dt\right) \quad \ldots (36)$$

As $\rho|_{t=0} = s_0$, as per Eq. (23), $z|_{t=0}$ is zero. Accordingly, Eq. (36) can be revised as:

$$\hat{h}_1 = \hat{h}_1\Big|_{t=0} + \frac{1}{\tau}\left(z + \int_0^t k_z z dt\right) \quad \ldots (37)$$

By substituting Eqs. (29), (34) and (37) into Eq. (28), the PPC and IDC-based guidance law are yielded as follows.

$$A_M = -R\left(\frac{2\dot{R}\dot{\lambda}}{R} + \frac{\dot{\rho}}{\rho}s_e - k\dot{e}_\lambda - \frac{\rho}{C}\left(k_z z + \hat{h}_1\Big|_{t=0} + \frac{1}{\tau}\left(z + \int_0^t k_z z dt\right)\right)\right) \quad \ldots (38)$$

In order to avoid A_m having large and discontinuous changes at the initial time, $\hat{h}_1\Big|_{t=0}$ is necessary to be predesigned. Assuming $A_M|_{t=0^-}$ is known, then, $A_M|_{t=0^+}$ can be subsequently determined from Eq. (38) as:

$$A_m|_{t=0^+} = A_m|_{t=0^-} + R|_{t=0^+}\ \hat{h}_1\Big|_{t=0} + \varepsilon|_{t=0^+} \quad \ldots (39)$$

https://doi.org/10.1017/aer.2019.121 Published online by Cambridge University Press

where $\varepsilon|_{t=0^+}$ is a small value. Then, $\hat{h}_1\Big|_{t=0}$ should be zeroed; then, Eq. (38) should be revised to:

$$A_M = -R\left(\frac{2\dot{R}\dot{\lambda}}{R} + \frac{\dot{\rho}}{\rho}s_e - k\dot{e}_\lambda - \frac{k_z z\rho}{C} - \frac{\rho}{C\tau}\left(z + \int_0^t k_z z dt\right)\right) \quad \ldots (40)$$

Then, the proposed guidance law (PIGL) which integrates PPC and IDC can be obtained from Eq. (40).

Next, the stability and robustness of the system from Eq. (24) has been analyzed by applying PIGL from Eq. (38).

By substituting Eq. (38) into Eq. (27), the derivative of z can be obtained as:

$$\dot{z} = -k_z z + \left(h_1 - \hat{h}_1\right) \quad \ldots (41)$$

Then $\tilde{h}_1 = h_1 - \hat{h}_1$ can be defined and the derivative of $\tilde{h}_1$ is obtained as

$$\dot{\tilde{h}}_1 = -\tau^{-1}\tilde{h}_1 + \dot{h}_1 \quad \ldots (42)$$

A Lyapunov function $v\left(z, \tilde{h}_1\right)$ can be constructed as

$$v\left(z, \tilde{h}_1\right) = \frac{1}{2}z^2 + \frac{1}{2}\tilde{h}_1^2 \quad \ldots (43)$$

Substituting Eqs. (41) and (42) into the derivative of $v\left(z, \tilde{h}_1\right)$, $\dot{v}\left(z, \tilde{h}_1\right)$ yields the following:

$$\begin{aligned}\dot{v}\left(z, \tilde{h}_1\right) &= -k_z z^2 + \tilde{h}_1 z - \tau^{-1}\tilde{h}_1^2 + \tilde{h}_1\dot{h}_1 \\ &\leq -\left(k_z - 1/2\right)z^2 - \left(\tau^{-1} - 1\right)\tilde{h}_1^2 + \dot{h}_1^2\end{aligned} \quad \ldots (44)$$

From Eq. (9) and Eq. (30), it can be seen that $\dot{h}_1^2$ is bounded. Therefore, the necessary conditions which assure $v\left(z, \tilde{h}_1\right)$ converges to a boundary region around zero are $k_z > 1/2$ and $0 < \tau < 1$. z is substantially bounded at $t = t_d$, and $s_e|_{t=t_d}$ could converge to a small region around s_d [21].

Remark 1. The proposed PIGL is only able to drive the desired sliding mode variable to a predesigned small region around its predesigned value at the desired time notwithstanding large sudden changes in guidance commands which can be avoided, and the dominated gain k_z in the guidance law can be loosely chosen.

3.2 SMC and IDC-based guidance law (SIGL)

PIGL is capable of controlling both the LOS angle and its rate to a small region without an abrupt command altering it under the unknown uncertainty induced by the target's maneuvers. However, it is not able to accurately drive the LOS angle and LOS angle rate to the desired value. Here, a SMC and IDC-based guidance law (SIGL) has been proposed to implement the final convergence of both the LOS angle and its rate.

The auxiliary variable σ [13] can be defined as:

$$\sigma = s_e + z_s, \quad z_s|_{t=t_0} = -\,s_e|_{t=t_0} \quad \ldots (45)$$

https://doi.org/10.1017/aer.2019.121 Published online by Cambridge University Press

Where, t_0 is the initial time when SMC and IDC-based guidance law are applied and the derivative of z_s is as follows:

$$\dot{z}_s = k_s s_e + l_s\,(t - t_0)\,sign(s_e) \quad \ldots (46)$$

where k_s is a positive value and l_s is a small positive value.

Consequently, by substituting Eqs. (12), (14) and (46) into the derivative of σ yields $\dot{\sigma}$ as follows.

$$\dot{\sigma} = -\frac{2\dot{R}\dot{\lambda} - h + A_M}{R} + k\dot{e}_\lambda + k_s s_e + l_s\,(t - t_0)\,sign(s_e) \quad \ldots (47)$$

A_M can be defined as:

$$A_M = -R(u_{eq} + u_1) \quad \ldots (48)$$

where

$$u_{eq} = \frac{2\dot{R}\dot{\lambda}}{R} - (k\dot{e}_\lambda + k_s s_e + l_s(t - t_0)sign(s_e)) \quad \ldots (49)$$

and h_1 can be defined as follows:

$$h_2 = \frac{h}{R} \quad \ldots (50)$$

Accordingly, substituting Eqs. (48), (49) and (50) into Eq. (47) yields h_2 as follows.

$$h_2 = \dot{\sigma} - u_1 \quad \ldots (51)$$

If h_2 is passed through a broadband filter $G_f(s)$ from Eq. (32), then, the dynamics of the estimate of h_2 is yielded as

$$\tau\dot{\hat{h}}_2 + \hat{h}_2 = \dot{\sigma} - u_1 \quad \ldots (52)$$

u_1 can be designed as:

$$u_1 = -k_\sigma \sigma - \hat{h}_2 \quad \ldots (53)$$

Substituting Eq. (53) into Eq. (52) yields $\dot{\hat{h}}_2$ as follows.

$$\dot{\hat{h}}_2 = \tau^{-1}\,(\dot{\sigma} + k_\sigma \sigma) \quad \ldots (54)$$

Integrating both sides of Eq. (54) yields $\hat{h}_2$ as follows.

$$\hat{h}_2 = \hat{h}_2\Big|_{t=t_0} + \frac{1}{\tau}\left(\sigma + \int_{t_0}^{t} k_\sigma \sigma\, dt\right) \quad \ldots (55)$$

https://doi.org/10.1017/aer.2019.121 Published online by Cambridge University Press

Accordingly, the SMC and IDC-based guidance law (SIGL) are yielded as follows

$$A_M = -R\Bigg(\frac{2\dot{R}\dot{\lambda}}{R} - (k\dot{e}_\lambda + k_s s_e + l_s(t-t_0)sign(s_e)) - \left(k_\sigma + \tfrac{1}{\tau}\right)\sigma - \hat{h}_2\Big|_{t=t_0} - \tfrac{1}{\tau}\int_{t_0}^{t} k_\sigma \sigma\, dt\Bigg) \quad \ldots (56)$$

Next, the stability and robustness of the system from Eq. (45) by applying SIGL from Eq. (56) has been analyzed.

Substituting Eq. (56) into Eq. (47), the derivative of σ is yielded as

$$\dot{\sigma} = -k_\sigma \sigma + \left(h_2 - \hat{h}_2\right) \quad \ldots (57)$$

Defining $\tilde{h}_2 = h_2 - \hat{h}_2$ and the derivative of $\tilde{h}_2$ can be written as:

$$\dot{\tilde{h}}_2 = -\tau^{-1}\tilde{h}_2 + \dot{h}_2 \quad \ldots (58)$$

A Lyapunov function $\nu\left(\sigma, \tilde{h}_2\right)$ can be constructed as

$$\nu\left(\sigma, \tilde{h}_2\right) = \frac{1}{2}\sigma^2 + \frac{1}{2}\tilde{h}_2^2 \quad \ldots (59)$$

Substituting Eq. (57) and Eq. (58) into the derivative of $\nu\left(\sigma, \tilde{h}_2\right)$ yields $\dot{\nu}\left(\sigma, \tilde{h}_2\right)$ as follows.

$$\begin{aligned}\dot{\nu}\left(\sigma, \tilde{h}_2\right) &= -k_\sigma \sigma^2 + \tilde{h}_1\sigma - \tau^{-1}\tilde{h}_2^2 + \tilde{h}_2\dot{h}_2 \\ &\leq -\left(k_\sigma - 1/2\right)\sigma^2 - \left(\tau^{-1} - 1\right)\tilde{h}_2^2 + \dot{h}_2^2\end{aligned} \quad \ldots (60)$$

As per Eqs. (9) and (50), $\dot{h}_2^2$ is bounded, the necessary conditions where $\nu\left(\sigma, \tilde{h}_2\right)$ converges to a boundary region are $k_\sigma > 1/2$ and $0 < \tau < 1$.

Furthermore, a Lyapunov function ν_{s_e} can be defined as

$$\nu_{s_e} = \frac{1}{2}s_e^2 \quad \ldots (61)$$

Substituting Eqs. (46) and (57) into the derivative of ν_{s_e} yields $\dot{\nu}_{s_e}$ as follows.

$$\begin{aligned}\dot{\nu}_{s_e} &= s_e\left(-k_s s_e - l_s(t-t_0)sign(s_e) - k_\sigma\sigma + \tilde{h}_2\right) \\ &\leq -2k_s V_{s_e} - \sqrt{2}\left(l_s(t-t_0) - |k_\sigma\sigma| - \left|\tilde{h}_2\right|\right)V_{s_e}^{1/2}\end{aligned} \quad \ldots (62)$$

Since $|\sigma|$ and $\left|\tilde{h}_2\right|$ are bounded, $|\sigma| \leq |\sigma|_{\max}$ and $\left|\tilde{h}_2\right| \leq \left|\tilde{h}_2\right|_{\max}$ can be defined. Theoretically, different values of l_s exist, if $t_f > t \geq t_s > t_0$, $l_s\,(t-t_0)|_{t>t_s} = \upsilon + |\sigma|_{\max} + \left|\tilde{h}_2\right|_{\max}$, where t_f denotes the terminal guidance time. Accordingly, if $t_f > t \geq t_s > t_0$, then Eq. (62) can be revised as follows:

$$\dot{\nu}_{s_e}\big|_{t>t_s} \leq -2k_s\nu_{s_e}\big|_{t>t_s} - \sqrt{2}\upsilon\nu_{s_e}^{1/2}\Big|_{t>t_s} \quad \ldots (63)$$

https://doi.org/10.1017/aer.2019.121 Published online by Cambridge University Press

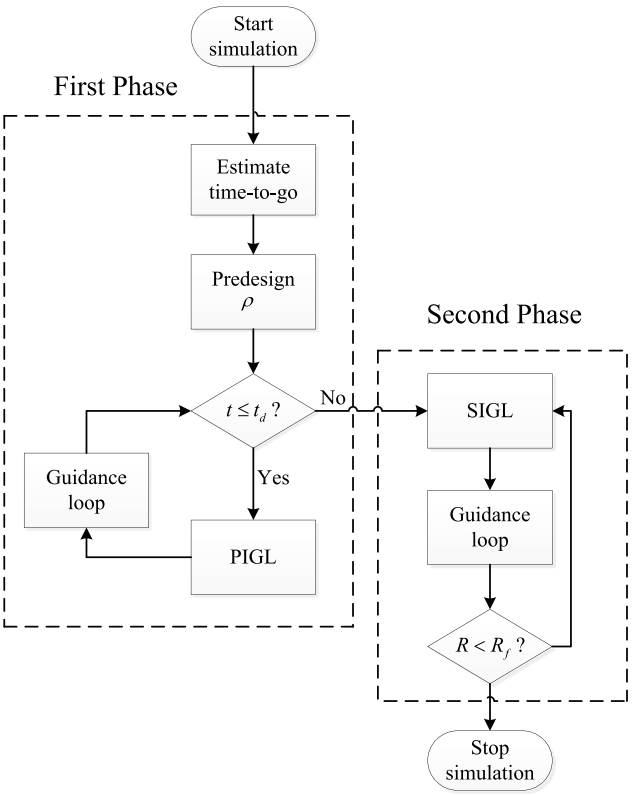

Figure 2. Hybrid guidance law scheme.

As per the literature[22], v_{s_e} will converge to zero in a finite time; consequently, s_e converges to zero in a finite time. Furthermore, e_λ and $\dot{e}_\lambda$ will asymptotically converge to zero.

Remark 2. The proposed SIGL with terminal LOS angle constraint, is able to guarantee the desired sliding mode variable's convergence to zero in a finite time and drive both the LOS angle and the LOS angle rate to asymptotically converge. However, the guidance command is still sensitive to the starting value of the sliding mode variable.

3.3 The hybrid strategy

Considering the strengths and weaknesses of both PIGL and SIGL, a hybrid guidance strategy has been proposed here to capture a non-cooperative maneuvering target without knowing the uncertainty h in advance. The guidance strategy for the terminal homing phase consists of two phases.

In the first phase, the PIGL guidance law is adopted to control s_e in a small predesigned range without large and abrupt changes of the guidance commands in a fixed time t_d, where $t_d = t_{go_0} - t_{switch}$. t_{go_0} is the initial estimated time-to-go between the missile and the target, and determined by $t_{go_0} \approx -R|_{t=0} \,/\, \dot{R}|_{t=0}$. t_{switch} is a predetermined time point, at which, the PIGL is shifted to SIGL. In order to achieve smooth switching, $u_{\rho d}$ is established as $-k_s s_d$.

https://doi.org/10.1017/aer.2019.121 Published online by Cambridge University Press

Table 1
Initial values of the missile and the target

Parameter	Value	Parameter	Value	Parameter	Value
$x_M\|_{t=0}$	0m	$y_M\|_{t=0}$	24000m	$x_T\|_{t=0}$	12000m
$y_T\|_{t=0}$	12000m	V_M	400m/s	V_T	200m/s
$\gamma_M\|_{t=0}$	$\pi/12$rad	$\gamma_T\|_{t=0}$	πrad	$A_M\|_{t=0}$	0m/s^2

In the second phase, SIGL is applied to guarantee that s_e converges to zero in a finite time in order to pursue high interception accuracy with reduced sensitivity to errors in the estimation of the time-to-go.

From the analysis of both phases, the time-to-go estimation will not be used as per PIGL in Eq. (40) and SIGL in Eq. (56) in the application process. The hybrid guidance law scheme has been shown in Fig. 2.

4.0 SIMULATION

In this section, a situation of the terminal homing phase for defensive missile has been examined. The first part contains a comparison between the proposed robust hybrid nonlinear guidance law and the other guidance laws. The second part includes a performance test of the proposed robust hybrid nonlinear guidance law.

4.1 Comparison with the other guidance laws

The initial simulation conditions have been provided in Table 1. The maneuvering acceleration profile of the target was assumed as $A_T = -4g\sin(\pi t/4)$, where $g = 9.8\text{m/s}^2$ denotes the value of the acceleration du to gravity. The desired terminal LOS angle was $\lambda_d = \pi/6$rad, and the upper bound of acceleration of interception missiles is assumed to be 20g. For comparison, another two guidance laws were introduced. One was the continuous impact angle homing guidance law in Ref.[5], named S Cont.-SMC for short. The other is a second order sliding mode guidance law with uncertainty and disturbance estimator in Ref.[6], named Est.-SMC for short.

Cont.-SMC is represented per the literature as[5]:

$$A_M = \frac{R}{\cos(\lambda - \gamma_M)}\left[-\frac{2\dot{R}\dot{\lambda}}{R} + \frac{q}{\eta p}\left|\dot{\lambda}\right|^{2-\frac{p}{q}} sgmf\left(\dot{\lambda}\right) + \frac{k_1}{R}s + \frac{k_2}{R}\left|s\right|^{\omega} sgmf\left(s\right)\right] \quad \ldots (64)$$

where

$$s = e_\lambda + \eta\left|\dot{e}_\lambda\right|^{\frac{p}{q}} sign(\dot{e}_\lambda) \quad \ldots (65)$$

$$sgmf(s) = 2\left(\frac{1}{1+\exp(-as)} - \frac{1}{2}\right), \quad a > 0 \quad \ldots (66)$$

Est.-SMC is represented per the literature as[6]:

$$A_M = u_e + u_s + \hat{h} \quad \ldots (67)$$

https://doi.org/10.1017/aer.2019.121 Published online by Cambridge University Press

where

$$u_e = -(k_3 + k_4 + 2)\dot{R}\dot{\lambda} - \frac{(k_4 + 1)k_3}{t_{go}}\dot{R}\,(\lambda - \lambda_d) \quad \ldots (68)$$

$$u_s = -R\,\{-b_1\,|\kappa|^{\alpha_1}\,sign(\kappa) + w\} \quad \ldots (69)$$

$$\hat{h} = (R\kappa + w_2)/\tau_m \quad \ldots (70)$$

$$\begin{cases} \kappa = s_b + m_z,\ m_z|_{t=0} = -\,s_b|_{t=0} \\ s_b = \dot{\lambda} + k_3\frac{\lambda - \lambda_d}{t_{go}} \\ \dot{m}_z = \frac{k_4 s_b}{t_{go}} \\ \dot{w} = -b_2\,|\kappa|^{\alpha_2}\,sign(\kappa) \\ \dot{w}_2 = -\dot{R}\kappa + u_s \end{cases} \quad \ldots (71)$$

The parameters of the proposed Hybrid guidance law were assigned as $k = 30$, $k_s = 1.0, l_s = 1.0 \times 10^{-3}, M_{\min} = -2, M_{\max} = 4, k_\sigma = k_z = 2, \tau = 0.05s, \beta = 0.01, t_{switch} = 8s$, $s_e|_{t=t_d} = s_0/50$.

The parameters for the Cont.-SMC guidance law were $\eta = 1$, $p = 21$, $q = 19$, $k_1 = 60$, $k_2 = 400$, $\omega = 0.5$, $a = 100$.

The values of the parameter for the Est.-SMC guidance law were $k_3 = 3$, $k_4 = 1.5$, $b_1 = 1$, $b_2 = 1$, $\alpha_1 = 0.7$, $\alpha_2 = 0.7$, $\tau_m = 0.05s$.

To avoid chattering in the guidance commands caused by the discontinuous signum function, a saturation function $sat(x)$ was used to address the problem as per the literature[14]:

$$sat(x) = \begin{cases} sign(x), & |x| > \vartheta \\ x/\vartheta, & |x| \le \vartheta \end{cases} \quad \ldots (72)$$

Where, ϑ is a small positive constant and was selected as 0.001. The simulation step was 2ms, and the simulation was terminated when $R \le R_f = 20$m.

The results of simulation have been shown in Fig. 3. The terminal guidance errors have been listed in Table 2. Figure 3(a) has shown the trajectories of the missile during the terminal homing interception phase. The curvatures of the trajectories at the beginning of the terminal homing phase generated by Cont.-SMC and Est.-SMC were greater than that for the Hybrid guidance law. Meanwhile, the commanded accelerations of the missile have been shown in Fig. 2(b). The largest acceleration in the initial homing phase determined by Hybrid guidance law was smaller than the other two guidance laws. Figure 3(c) and (d) indicate that the terminal LOS angle and its rate finally converged rapidly to the desired value and around zero, respectively. During the convergence phase, the LOS angle and the LOS angle rate yielded by the Hybrid guidance law were not affected by target's maneuvers, while those from the other two guidance law were deeply affected by target's maneuver. Compared with Cont.-SMC and Est.-SMC, the values of the LOS angle and the LOS angle rate reached zero more quickly and could stay in small regions around zero. In Fig. 3(e), the sliding mode variable determined by the hybrid guidance law could be driven into the predesigned region at a fixed time and converged to zero to pursue high terminal interception precision. Even though the time-to-go is not used by the Hybrid guidance law, the terminal interception precision can be guaranteed as the performance of the Est.-SMC guidance law.

https://doi.org/10.1017/aer.2019.121 Published online by Cambridge University Press

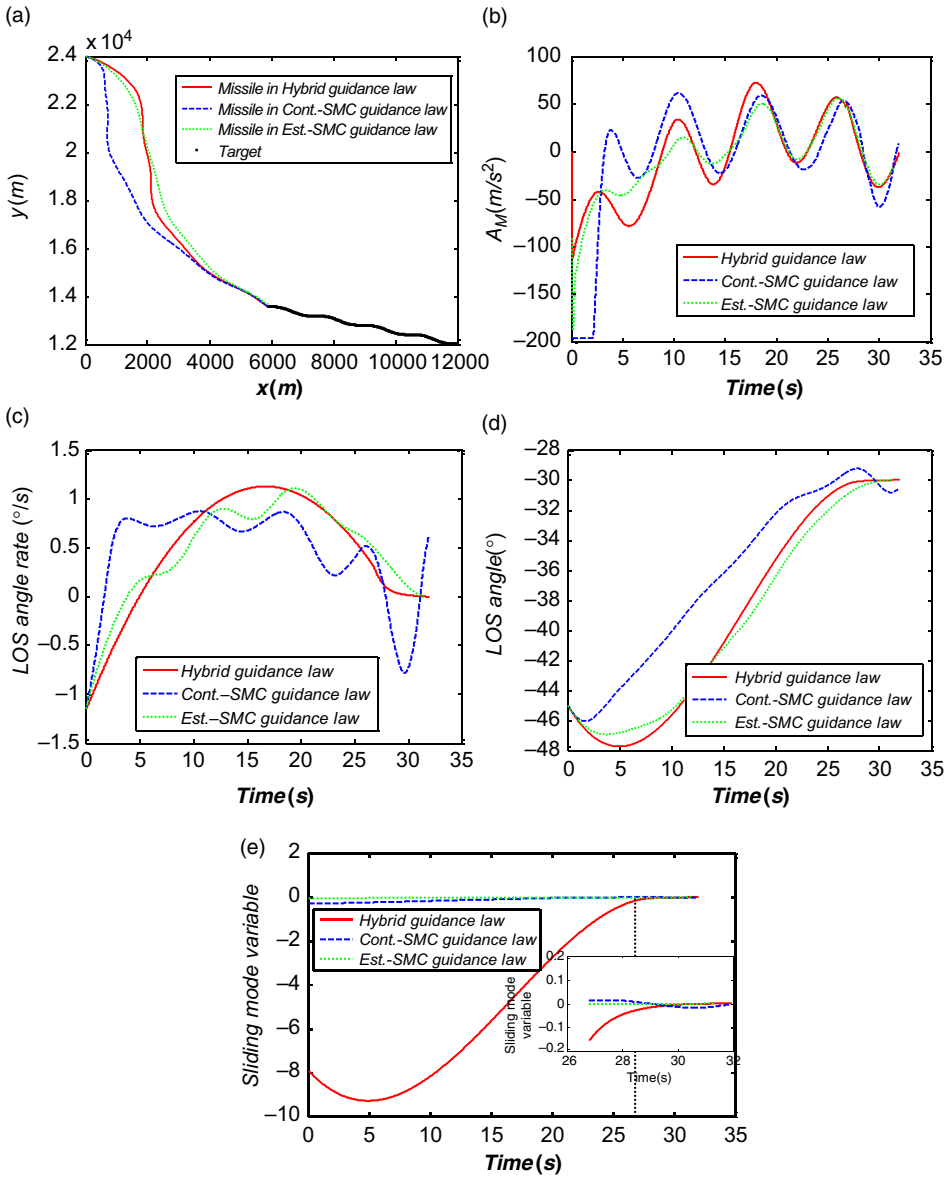

Figure 3. Comparison results from the Hybrid guidance law, the Cont.-SMC guidance law and the Est.-SMC guidance law: a) interception trajectories, b) the accelerations the missile achieved, c) the LOS angle rate, d) the LOS angle, e) the sliding mode variables.

4.2 Performance test

In order to verify the robustness and performance of the proposed guidance law, Monte Carlo simulation with 100 cases was then carried out. The dispersion of the parameters for the Monte Carlo simulation has been listed in Table 3. Moreover, the dominated control gain k_z, assumed to be loosely chosen in boundary regions, was dealt with as an uncertainty.

Figure 4(a) has shown the acceleration commands of the missile under different initial states and for various values of the control gain k_z. It also indicates that large abrupt changes

https://doi.org/10.1017/aer.2019.121 Published online by Cambridge University Press

Table 2
Terminal guidance errors

Guidance law	Hybrid guidance law	Cont.-SMC guidance law	Est.-SMC guidance law
Terminal LOS angle error $(^\circ)$	0.0001	−0.5631	0.0007
Terminal LOS anglerate error $(^\circ/s)$	−0.0007	0.6112	−0.0088
Terminal zero-effort miss $\lvert \dot{e}r^2/\dot{r} \rvert$, m	0.0001	0.0075	0.0001
Interception time, s	31.962	31.874	31.380

Table 3
Lower and upper bounds for the uncertainty parameters

Parameters	Lower value	Upper value
V_M(m/s)	380	420
V_T(m/s)	180	220
$\gamma_M\vert_{t=0}$ (rad)	$-\pi/18$	$-\pi/6$
$\gamma_t\vert_{t=0}$ (rad)	$8\pi/9$	π
k_z	2	20

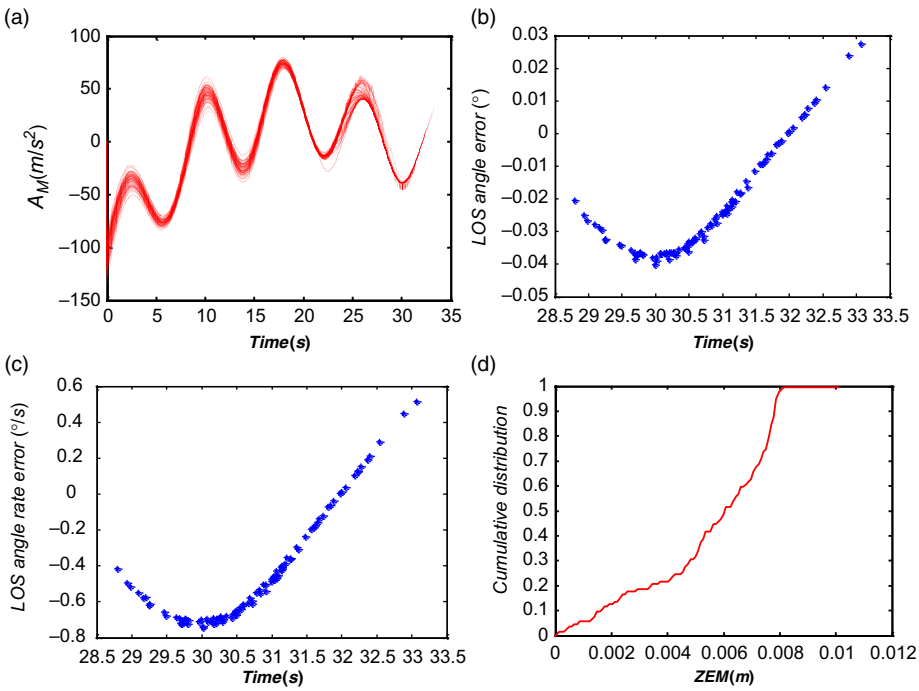

Figure 4. Monte Carlo results with the Hybrid guidance law: (a) Acceleration the missile achieved, (b) Scatter diagram of the terminal LOS angle error, (c) Scatter diagram of the terminal LOS angle rate error, (d) Cumulative distribution of zero-effort miss.

https://doi.org/10.1017/aer.2019.121 Published online by Cambridge University Press

in the beginning period were eliminated notwithstanding the initial states, and that the control gain k_z varied. Therefore, it demonstrated one critical advantage where the yielded guidance commands were insensitive to the initial state errors between the initial states and the desired states as well as the uncertainty caused by the target's maneuvers. Figure 4(b) and (c) have depicted the scatter of the terminal LOS angle error and the LOS angle rate error of the missile, they have demonstrated that the proposed guidance law has a good robustness in guaranteeing the convergent accuracy of the LOS angle and the LOS angle rate errors. Figure 4(d) has depicted the zero-effort miss between the missile and the target; it reflects that fact that the proposed robust hybrid nonlinear guidance law can guide the missile to achieve high interception accuracy. Subsequently, another advantage, where it loosely chooses the control gain k_z without acquiring the uncertainties in advance, has been demonstrated by this numerical simulation.

5.0 CONCLUSIONS

This paper has proposed a new robust hybrid nonlinear guidance law to intercept a non-cooperative maneuvering target, which possesses the advantages of two sub-guidance laws: PIGL and SIGL. The proposed guidance law provides a tunable method to drive the LOS angle and LOS angle rate-based sliding mode variable to a small predesigned region within a fixed time, and it can eliminate large acceleration changes when the guidance law is activated and target perform a significant maneuver. Accordingly, high terminal interception precision can be assured notwithstanding that the time-to-go of the missile is not used by the hybrid guidance law in the application process. Moreover, the robustness of both the proposed sub-guidance laws has been proved explicitly.

REFERENCES

1. SONG, H., ZHANG, T., ZHANG, G. and LU, C. Integrated interceptor guidance and control with prescribed performance, *International Journal of Robust and Nonlinear Control*, 2015, **25**, (16), pp 3179–3194.
2. WEISS, G. and RUSNAK, I. All-Aspect Three-Dimensional Guidance Law Based on Feedback Linearization, *Journal of Guidance, Control, and Dynamics*, 2015, **38**, (12), pp 1–8.
3. YANG, C.-D. and CHEN, H.-Y. Nonlinear H robust guidance law for homing missiles, *Journal of Guidance, Control, and Dynamics*, 1998, **21**, (6), pp 882–890.
4. PENGLEI, Z., CHEN, W. and YU, W. Guidance law for intercepting target with multiple no-fly zone constraints, *Aeronautical Journal*, 2017, **121**, (1244), pp 1479–1501.
5. HE, S. and LIN, D. Sliding mode-based continuous guidance law with terminal angle constraint, *The Aeronautical Journal*, 2016, **120**, (1229), pp 1175–1195.
6. YAMASAKI, T., BALAKRISHNAN, S., TAKANO, H. and YAMAGUCHI, I. Sliding mode-based intercept guidance with uncertainty and disturbance compensation, *Journal of the Franklin Institute*, 2015, **352**, (11), pp 5145–5172.
7. SHIN, H.S., LI, K.B. and TSOURDOS, A. A New Three-Dimensional Sliding Mode Guidance Law Variation with Finite Time Convergence, *IEEE Transactions on Aerospace & Electronic Systems*, 2017, **53**, (5), pp 2221–2232.
8. SHIMA, T. Intercept-angle guidance, *Journal of Guidance, Control, and Dynamics*, 2011, **34**, (2), pp 484–492.
9. GINOYA, D., SHENDGE, P. and PHADKE, S. Sliding mode control for mismatched uncertain systems using an extended disturbance observer, *IEEE Transactions on Industrial Electronics*, 2014, **4**, (61), pp 1983–1992.
10. GUO, Z., GUO, J. and ZHOU, J. Adaptive attitude tracking control for hypersonic reentry vehicles via sliding mode-based coupling effect-triggered approach, *Aerospace Science and Technology*, 2018, **78**, pp 228–240.

https://doi.org/10.1017/aer.2019.121 Published online by Cambridge University Press

11. ZHAO, Y., SHENG, Y. and LIU, X. Sliding mode control based guidance law with impact angle constraint, *Chinese Journal of Aeronautics*, 2014, **27**, (1), pp 145–152.
12. LIN, C.-L., HSIEH, S.-L. and LIN, Y.-P. Trajectory estimation based on extended state observer with Fal-filter, *Aeronautical Journal*, 2015, **119**, (1218), pp 1017–1031.
13. PHADKE, S. and TALOLE, S. Sliding mode and inertial delay control based missile guidance, *IEEE Transactions on Aerospace and Electronic Systems*, 2012, **48**, (4), pp 3331–3346.
14. HE, S., LIN, D. and WANG, J. Robust terminal angle constraint guidance law with autopilot lag for intercepting maneuvering targets, *Nonlinear Dynamics*, 2015, **81**, (1–2), pp 881–892.
15. SHIN, H.-S., LEE, J.-I. and TSOURDOS, A. A New Impact Angle Control Guidance Law to Reduce Sensitivity on Initial Errors, Advances in Aerospace Guidance, Navigation and Control, 2015, Springer, Cham.
16. LIU, J. and WANG, X. *Advanced sliding mode control for mechanical systems*, Springer, Heidelberg, Berlin, Germany, 2012.
17. LYU, S. and ZHU, Z.H. Two-dimensional Continuous Terminal Interception Guidance Law with Predefined Convergence Performance, *IEEE Access*, 2018, **6**, pp 46771–46780.
18. LYU, S., ZHU, Z.H., TANG, S. and YAN, X. Prescribed performance slide mode guidance law with terminal line-of-sight angle constraint against maneuvering targets, *Nonlinear Dynamics*, 2017, **88**, (3), pp 2101–2110.
19. GRINFELD, N. and BEN-ASHER, J.Z. Minimal-Jerk Missile Guidance Law, *Journal of Guidance, Control, and Dynamics*, 2015, **38**, (8), pp 1–6.
20. BRYSON, A.E., HO, Y.C., SIOURIS, G.M. Applied optimal control: optimization, estimation and control, *IEEE Transactions on Systems Man and Cybernetics*, 1979, **9**, (6), pp 366–367.
21. BECHLIOULIS, C.P. and ROVITHAKIS, G.A. Adaptive control with guaranteed transient and steady state tracking error bounds for strict feedback systems, *Automatica*, 2009, **45**, (2), pp 532–538.
22. HONG, Y., HUANG, J. and XU, Y. On an output feedback finite-time stabilization problem, *IEEE Transactions on Automatic Control*, 2001, **46**, (2), pp 305–319.

https://doi.org/10.1017/aer.2019.121 Published online by Cambridge University Press